

The Open University's repository of research publications and other research outputs

Lanthanide Ionization Energies and the Sub-Shell Break. Part 2. The Third and Fourth Ionization Energies

Journal Item

How to cite:

Johnson, David A. and Nelson, Peter G. (2017). Lanthanide Ionization Energies and the Sub-Shell Break. Part 2. The Third and Fourth Ionization Energies. *Journal of Physical and Chemical Reference Data*, 46(1), article no. 013109.

For guidance on citations see [FAQs](#).

© 2017 AIP Publishing LLC



<https://creativecommons.org/licenses/by-nc-nd/4.0/>

Version: Version of Record

Link(s) to article on publisher's website:
<http://dx.doi.org/doi:10.1063/1.4977959>

Copyright and Moral Rights for the articles on this site are retained by the individual authors and/or other copyright owners. For more information on Open Research Online's data [policy](#) on reuse of materials please consult the policies page.

Lanthanide Ionization Energies and the Sub-Shell Break. Part 2. The Third and Fourth Ionization Energies

David A. JohnsonPeter G. Nelson

Citation: [Journal of Physical and Chemical Reference Data](#) **46**, 013109 (2017); doi: 10.1063/1.4977959

View online: <http://dx.doi.org/10.1063/1.4977959>

View Table of Contents: <http://aip.scitation.org/toc/jpr/46/1>

Published by the [American Institute of Physics](#)

Lanthanide Ionization Energies and the Sub-Shell Break. Part 2. The Third and Fourth Ionization Energies

David A. Johnson^{a)}

Department of Chemistry, The Open University, Milton Keynes MK7 6AA, England

Peter G. Nelson

Department of Chemistry, University of Hull, Hull HU6 7RX, England

(Received 5 August 2016; accepted 21 February 2017; published online 30 March 2017)

By interpolating a $4f^q6s \rightarrow 4f^{q+1}7s$ transition within the sequence $f^1 \rightarrow f^{14}$ rather than between f^0 and f^{14} , revised third and fourth ionization energies of the lanthanides have been obtained. The revised values, together with the second ionization energies calculated in a previous paper, are used to calculate values of the standard enthalpies of formation of the gaseous tripositive ions, $\Delta_f H^\ominus(M^{3+}, g)$, and of the lattice and hydration enthalpies of some lanthanide compounds and ions in the trivalent and tetravalent states. The displacements of f^0 values from nearly smooth $f^1 \rightarrow f^{14}$ variations exceed 30 kJ mol^{-1} and indicate substantial subshell breaks. © 2017 AIP Publishing LLC for the National Institute of Standards and Technology. [<http://dx.doi.org/10.1063/1.4977959>]

Key words: lanthanides; ionization energies; thermochemical properties; tetrad effect.

CONTENTS

1. Introduction	2	2. Calculation of n^* and $T(4f^q6s)$ in Ln IV spectra from estimated and experimental values of ΔT and Δn^*	3
2. The Values of Δn^*	2	3. Data used to estimate the $4f^q5d \rightarrow 4f^q6s$ transition energy in Nd III, Pm III, and Sm III	4
3. The Values of ΔT	3	4. Experimental data used to estimate unknown values of $E(4f^q6s)$ in Ln IV spectra	5
4. The values of $T(4f^q6s)$	3	5. Values of the Racah parameter G_3 for the configuration $4f^q6s$ in Ln III and Ln IV spectra	6
5. The Values of $E(4f^q6s)$ in Ln III	4	6. Values of the Racah parameter $G_3(4f^q7s)$ that were used in calculating the ΔT values plotted in Figs. 1 and 2	6
6. The Values of $E(4f^q6s)$ in Ln IV	5	7. Calculation of I_3 using Fig. 4 for the estimation of unknown values of $E(4f^q6s)$	7
7. The Values of G_3 and δ	6	8. Calculation of I_4 from the experimental values of $E(4f^q6s)$ and estimated values obtained using Fig. 5	7
8. The Ionization Energies	6	9. Three sets of third and fourth ionization energies: Columns 2 and 6, Sugar and Reader (1973); columns 3 and 7, current NIST recommendations; columns 4 and 8, this work	8
8.1. Third ionization energies	7	10. Thermodynamic data on lanthanide compounds and ions at 298.15 K; q is the number of 4f electrons in the gaseous tripositive ion	9
8.2. Fourth ionization energies	8	11. Calculation of the lattice enthalpies of lanthanide and hafnium dioxides with the fluorite structure; q is the number of 4f electrons in the gaseous tetrapositive ion	11
8.3. The standard enthalpies of formation of gaseous tripositive ions	9		
8.4. Irregularities in the $4f^q5d \rightarrow 4f^q6s$ transition in Ln III	10		
8.5. Lattice enthalpies and hydration enthalpies of trivalent compounds and ions	10		
8.6. Lattice enthalpies of tetravalent lanthanide oxides	11		
9. Conclusion	12		
Acknowledgments	12		
10. References	12		

List of Tables

1. Calculation of n^* and $T(4f^q6s)$ in Ln III spectra from estimated and experimental values of ΔT and Δn^*	2
-------------------------------------------------------------------------------------------------------------------------------------------	---

List of Figures

1. The energy difference, ΔT , between the $4f^q$ parent levels of the $4f^q6s$ and $4f^q7s$ configurations in lanthanide III spectra plotted against q	3
-----------------------------------------------------------------------------------------------------------------------------------------------------------------------------	---

^{a)} Author to whom correspondence should be addressed; electronic mail: daj_jih@btinternet.com.

2. The energy difference, ΔT , between the $4f^q$ parent levels of the $4f^q6s$ and $4f^q7s$ configurations in lanthanide IV and Hf IV spectra plotted against q 3
3. Variations in the observed values of the transition between the lowest levels of the $4f^q5d$ and $4f^q6s$ configurations in lanthanide II and lanthanide III spectra plotted against q 4
4. Experimentally determined differences between the lowest levels of the $4f^q5d$ and $4f^q6s$ configurations in Ln III spectra plotted against their isoelectronic Ln II counterparts 5
5. Differences between the lowest levels of the $4f^{q+1}$ and $4f^q6s$ configurations in the Ln IV spectra plotted against their Ln III counterparts 6
6. The fourth ionization energies of the lanthanides plotted against the third ionization energies for isoelectronic transitions of the type $\{Xe\}4f^n \rightarrow \{Xe\}4f^{n-1}$ 8
7. Plot of $\Delta_r H^\ominus(M^{3+},g)$ for lanthanide elements against q where q is the number of $4f$ electrons in the gaseous tripositive ion 10
8. Variations in the energy of the transition between the lowest levels of the $4f^q5d$ and $4f^q6s$ configurations in lanthanide III spectra plotted against q 10
9. The lattice and hydration enthalpies of some isostructural trivalent and tetravalent lanthanide compounds and ions plotted against q , the number of $4f$ electrons in the free ion 11

1. Introduction

In a recent work,¹ we revised the second ionization energies obtained in a seminal paper by Sugar and Reader.² Improved accuracy was achieved in this revision by avoiding the influence of a possible subshell break and using more recent auxiliary data. Here we update, in a similar way, the third and fourth ionization energies obtained in a later paper³ by the same authors. This later paper is the source of most recommended values of lanthanide third and fourth ionization energies on the invaluable NIST Atomic Spectra Database website.⁴ Throughout, we shall be concerned with the third and fourth spectra, M III and M IV, of two series of atoms, M, in which the ion generated in the ionization limit has the ground state configuration $\{Xe\}4f^q$. This defines q and sets up the M III series as La \rightarrow Lu and the M IV series as Ce \rightarrow Hf, which both begin at $q = 0$ and end when $q = 14$.

As in the first paper, the method relies on a smooth variation in the energy difference, ΔT , between the unperturbed centers of gravity of the lowest pairs of levels of the $4f^q6s$ and $4f^q7s$ configurations. These lowest pairs arise from the same $4f^q$ parent state. Unknown values are obtained by interpolation of the smooth variation established by using the limited number of cases in which the necessary spectroscopic data are available for both the $4f^q6s$ and $4f^q7s$ levels. The ΔT values are then expressed by a Rydberg-Ritz formula

$$\Delta T = z^2 R \{ [1/n^*(6s)]^2 - [1/(n^*(6s) + \Delta n^*)]^2 \}, \quad (1)$$

where z is the charge of the ion that is formed during ionization, n^* is the effective principal quantum number, and R the Rydberg constant. Sugar and Reader³ used the value $\Delta n^* = 1.048$ for both series of elements with an estimated uncertainty of ± 0.002 . Each value of ΔT then yields a value of $n^*(6s)$ that provides $T(4f^q6s)$, the amount by which the unperturbed center of gravity of the lowest $4f^q6s$ pair lies below the ionization threshold. A small correction, denoted δ , converts this figure to the amount by which the lowest level of the $4f^q6s$ configuration (the lowest level of the lowest pair) lies below the ionization threshold and, if the excitation energy of that lowest level can be determined, the third and fourth ionization energies follow. In Secs. 2–9, we examine the steps

in the calculation in more detail, paying attention to the way in which Sugar and Reader's method has been revised.

2. The Values of Δn^*

In Paper I,¹ we calculated and surveyed the available experimental data on Δn^* for Ln II, Ln III, and Ln IV spectra and then used them to estimate unknown values for all three series. The values used here for the Ln III and Ln IV series appear in the fourth columns of Tables 1 and 2. They are the averages of the values provided by methods A and B in Table 2 of Paper I. As noted above, Sugar and Reader³ took $\Delta n^* = 1.048 \pm 0.002$ for both these series; our estimated values for Ln III differ from this by less than 0.003 and in most cases by less than 0.001. In the Ln IV series, our values are lower than 1.048 but at most by 0.004.

In Paper I, we also derived an uncertainty in our estimated values of Δn^* for all three series. This was ± 0.0052 at the level of two standard deviations, a convention that is also used for uncertainties derived in the present paper. In the Ln III

TABLE 1. Calculation of n^* and $T(4f^q6s)$ in Ln III spectra from estimated and experimental values of ΔT and Δn^* . Figures estimated by interpolation from Fig. 1 are in parentheses

q	Spectrum	$\Delta T/\text{cm}^{-1}$	Δn^*	n^*	$T(4f^q6s)/\text{cm}^{-1}$
0	La III	68 756 ^a	1.049 45	2.6458	141 086
1	Ce III	70 245 ^a	1.048 18	2.6233	143 516
2	Pr III	71 601 ^b	1.047 02	2.6034	145 719
3	Nd III	(72 833) ^c	1.047 6	2.5867	147 606
4	Pm III	(74 109) ^c	1.047 7	2.5695	149 589
5	Sm III	(75 381) ^c	1.047 8	2.5527	151 564
6	Eu III	(76 650) ^c	1.047 9	2.5363	153 531
7	Gd III	77 883 ^a	1.048 0	2.5208	155 425
8	Tb III	(79 180) ^c	1.047 6	2.5045	157 454
9	Dy III	(80 441) ^c	1.047 2	2.4890	159 422
10	Ho III	(81 699) ^c	1.046 9	2.4739	161 374
11	Er III	82 977 ^a	1.046 5	2.4589	163 348
12	Tm III	(84 211) ^c	1.046 1	2.4446	165 265
13	Yb III	85 475 ^a	1.045 3	2.4301	167 243
14	Lu III	86 681 ^a	1.045 65	2.4171	169 047

^aFrom Eq. (2) using experimental ΔE values^{4–6} and G_3 from Tables 5 and 6.

^bFrom Sugar and Reader's analysis³ (see Sec. 7).

^cBy interpolation in Fig. 1.

TABLE 2. Calculation of n^* and $T(4f^q6s)$ in Ln IV spectra from estimated and experimental values of ΔT and Δn^* . Figures estimated by interpolation from Fig. 2 are in parentheses

q	Spectrum	$\Delta T/\text{cm}^{-1}$	Δn^*	n^*	$T(4f^q6s)/\text{cm}^{-1}$
0	Ce IV	96 900 ^a	1.03741	2.8842	211 069
1	Pr IV	99 240 ^a	1.0463	2.8638	214 086
2	Nd IV	(100 983) ^b	1.0456	2.8444	217 017
3	Pm IV	(102 725) ^b	1.0457	2.8260	219 852
4	Sm IV	(104 466) ^b	1.0458	2.8079	222 695
5	Eu IV	(106 206) ^b	1.0460	2.7904	225 497
6	Gd IV	(107 945) ^b	1.0461	2.7731	228 320
7	Tb IV	(109 683) ^b	1.0462	2.7563	231 111
8	Dy IV	(111 420) ^b	1.0458	2.7395	233 955
9	Ho IV	(113 157) ^b	1.0454	2.7230	236 799
10	Er IV	(114 892) ^b	1.0450	2.7069	239 624
11	Tm IV	(116 626) ^b	1.0446	2.6911	242 446
12	Yb IV	118 386 ^a	1.0443	2.6755	245 281
13	Lu IV	12 0045 ^a	1.0440	2.6611	247 943
14	Hf IV	12 1846 ^a	1.0443	2.6461	250 762

^aFrom Eq. (2) using experimental ΔE values^{4,7,19,20} and G_3 from Tables 5 and 6.

^bBy interpolation in Fig. 2.

series, it is equivalent to a contribution of $\pm 400 \text{ cm}^{-1}$ to the uncertainty in the ionization energy. For the Ln IV series, the contribution is $\pm 600 \text{ cm}^{-1}$.

3. The Values of ΔT

Since 1973, $4f^q6s$ and $4f^q7s$ levels in the spectra of Gd III,⁵ Er III (Ref. 6), and Yb IV (Ref. 7) have become available. This means that, in the case of Ln III spectra, we have seven values of ΔT whereas Sugar and Reader had five; with Ln IV, there are now five rather than four. However, because of the possibility of a subshell break, we reject the La III and Ce IV values which visibly reduce the goodness of fit when ΔT is plotted against q .

ΔT is equal to the separation of the lowest levels of the $4f^q6s$ and $4f^q7s$ configurations after each lowest level has been corrected by the quantity, δ . As in Paper I, Judd's formulae^{8,9} were used to calculate the values of δ , which depend on the parameter G_3 . For non-zero values of $G_3(4f^q6s)$ in Ln III spectra, Sugar and Reader assumed $G_3 = 310 \text{ cm}^{-1}$; for the Ln IV spectra they took $G_3 = 410 \text{ cm}^{-1}$. We, however, have tried to calculate individual values where the available data permit. We give a full account of this in Sec. 7; here we merely direct attention to a useful result of Judd's formulae. If ΔE is the separation of the lowest levels of the configurations $4f^q6s$ and $4f^q7s$, and S_1 is the spin quantum number of the $4f^q$ core,

$$\Delta T = \Delta E - S_1 \{G_3(4f^q6s) - G_3(4f^q7s)\}. \quad (2)$$

Our six selected experimental values for Ln III are plotted against q in Fig. 1, and the four for Ln IV in Fig. 2. The values are among those shown in column 3 of Tables 1 and 2. None of the ten selected points deviate from the two fitted curves by more than 50 cm^{-1} . At $q = 0$, the displacement of the lanthanum III point from the curve is about 240 cm^{-1} ; that of cerium IV by nearly 600 cm^{-1} . By using the interpolation equation for Ln III, estimated values of ΔT can be obtained for Nd III, Pm III, Sm III, Eu III, Tb III, Dy III, Ho III, and Tm III;

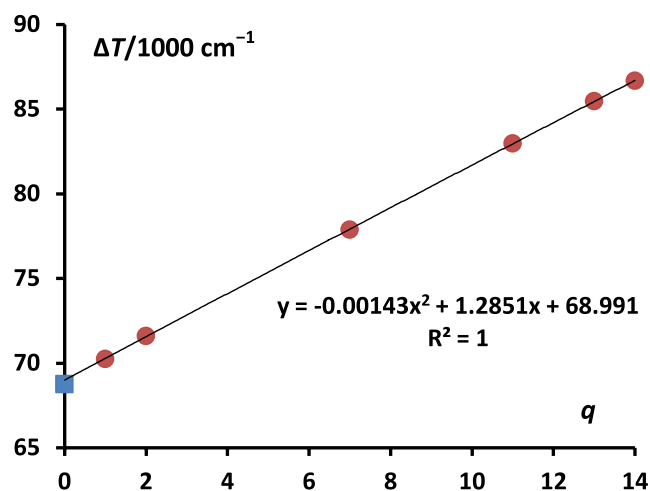


FIG. 1. The energy difference, ΔT , between the $4f^q$ parent levels of the $4f^q6s$ and $4f^q7s$ configurations in lanthanide III spectra plotted against q . Points in the range $q = 1 \rightarrow 14$ are marked with dark red circles; the $q = 0$ point is marked with a blue square (a linear fit gives $y = 1.2640x + 69.031$).

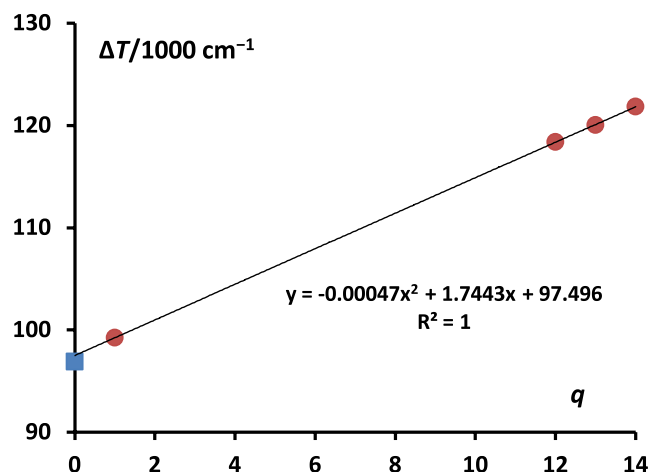


FIG. 2. The energy difference, ΔT , between the $4f^q$ parent levels of the $4f^q6s$ and $4f^q7s$ configurations in lanthanide IV and Hf IV spectra plotted against q . Points in the range $q = 1 \rightarrow 14$ are marked with dark red circles; the $q = 0$ point is marked with a blue square (a linear fit gives $y = 1.7376x + 97.504$).

the equation for Ln IV provides estimates of ΔT for the sequence Nd IV–Tm IV. These too appear in column 3 of Tables 1 and 2. For the uncertainty in the ΔT values, we note that doubling the standard deviation of the separations of the fitted points from the curves in Figs. 1 and 2 gives $\pm 70 \text{ cm}^{-1}$ in both cases. They transmit uncertainties of $\pm 110 \text{ cm}^{-1}$ to both the third and the fourth ionization energies.

4. The values of $T(4f^q6s)$

When inserted into Eq. (1), the estimated and experimental values of ΔT and Δn^* provide, first, values of $n^*(6s)$ for each element. The $n^*(6s)$ values in turn then yield $T(4f^q6s)$, the amount by which the unperturbed center of gravity of the lowest $4f^q6s$ pair lies below the ionization threshold of the sequence $4f^qns$. This threshold is the lowest level of the

configuration $4f^q$. The results of the calculations appear in Tables 1 and 2. In the Ln III spectra, the uncertainties in Δn^* and ΔT that we have already discussed contribute a combined uncertainty of $\pm 420 \text{ cm}^{-1}$ to $T(4f^q6s)$. In the Ln IV spectra, the figure is $\pm 620 \text{ cm}^{-1}$.

We now consider the calculation of the values of $E(4f^q6s)$. Because the method used for Ln III spectra differs from that applied to Ln IV, we have separate sections on the two types of spectra.

5. The Values of $E(4f^q6s)$ in Ln III

$E(4f^q6s)$ is the energy of the lowest level of the $4f^q6s$ configuration relative to the ground state of the dipositive ion. It is one of a pair, there being a higher partner level arising from the same $4f^q$ parent. The amount by which the lower level lies below the ionization threshold can be found by adding δ , its separation from the unperturbed center of gravity of the pair, to $T(4f^q6s)$. Thus, if the lowest level of the $4f^q6s$ configuration has been located in the Ln III spectrum, the third ionization energy is obtained as the sum $\{E(4f^q6s) + T(4f^q6s) + \delta\}$.

In their paper in 1973, Sugar and Reader had available ten experimental values of $E(4f^q6s)$: the missing values were those of neodymium, promethium, samarium, europium, and dysprosium. Sugar and Reader obtained estimates of their five missing values by using what they called the system difference (SD), the difference between the lowest levels of the configurations $4f^q5d$ and $4f^{q+1}$. Estimates of this quantity for the third spectra, Ln III, made by Martin¹⁰ allowed them to calculate ten values of the transition energy $4f^q5d \rightarrow 4f^q6s$ from their ten experimental values of $E(4f^q6s)$. They plotted these values against the atomic number and, by bridging the gaps with straight lines, obtained estimates for the energy of the $4f^q5d \rightarrow 4f^q6s$ transition in neodymium, promethium, samarium, europium, and dysprosium. Martin's SD estimates then allowed calculation of the five missing values of $E(4f^q6s)$.

Since 1973, experimental values of $E(4f^q6s)$ for europium¹¹ and dysprosium¹² have become available and there are now experimental data on the SD for all Ln III spectra except those of promethium and samarium. The twelve experimental values of $E(4f^q6s)$ are the figures without parentheses in column 5 of Table 7. The three values in parentheses have been obtained by a modification of the estimation method used by Sugar and Reader.

The upper plot in Fig. 3 shows the twelve experimental values of the $4f^q5d \rightarrow 4f^q6s$ transition energy in lanthanide III spectra plotted against q . Following Sugar and Reader, the missing values in neodymium, promethium, and samarium could be estimated by bridging the gap with a straight line. However, we have used a different method. The lower plot in Fig. 3 shows the $4f^q5d \rightarrow 4f^q6s$ transition energy for the iso-electronic lanthanide II spectra. The latter comprise a complete set and, as noted by Brewer,¹³ the two variations seem very similar. We have therefore estimated missing values in the lanthanide III spectra from the smooth curve obtained when the known Ln III values are plotted against their iso-electronic Ln II

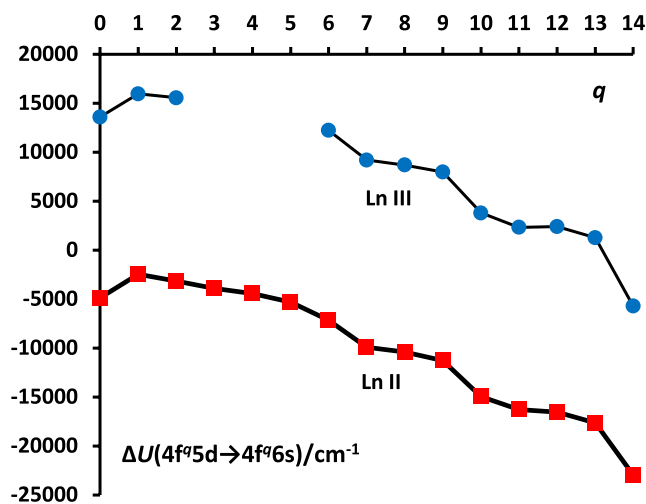


FIG. 3. Variations in the observed values of the transition between the lowest levels of the $4f^q5d$ and $4f^q6s$ configurations in lanthanide II and lanthanide III spectra plotted against q .

counterparts. The required transitions were chosen by first selecting those between the lowest levels of the two configurations. In all but two cases they then fulfilled a second requirement: that the spectroscopic designation of the initial and of the final states should be the same. The two cases in question were Gd II and Dy II, where $^8G_{13/2}$ in $4f^85d$ and $^6H_{15/2}$ in $4f^{10}5d$ were chosen so that they matched the lowest levels in Tb III and Ho III. The disruptions in level ordering are due to departures from LS coupling but the matched levels have similar percentage compositions and the adjustments are small: 22 and 106 cm^{-1} , respectively.

The required data are shown in Table 3 and the plot appears in Fig. 4. The terminal point, Yb II/Lu III, has been omitted because it is so remote from the region within which we need to interpolate.

When inserted into the polynomial fit of Fig. 4, the Pr II, Nd II, and Pm II figures in Table 3 give 14 872, 14 394, and 13 598 cm^{-1} for the $4f^q5d \rightarrow 4f^q6s$ transition energy in Nd III,

TABLE 3. Data used to estimate the $4f^q5d \rightarrow 4f^q6s$ transition energy in Nd III, Pm III, and Sm III

q	Ln II{ $4f^q5d \rightarrow 4f^q6s$ } ^a	Ln III{ $4f^q5d \rightarrow 4f^q6s$ } ^a
	cm^{-1}	
1	-2 451	15 959
2	-3 158	15 553
3	-3 893	
4	-4 438	
5	-5 332	
6	-7 135	12 240
7	-9 923	9 195
8	-10 397 ^b	8 704
9	-11 262	7 980
10	-14 952 ^b	3 791
11	-16 282	2 340
12	-16 553	2 405
13	-17 625	1 270
14	-22 961	-5 708

^aUnless otherwise stated, transitions occur between the lowest levels of the configurations; data are from Ref. 4.

^bIncludes small adjustments described in Sec. 5.

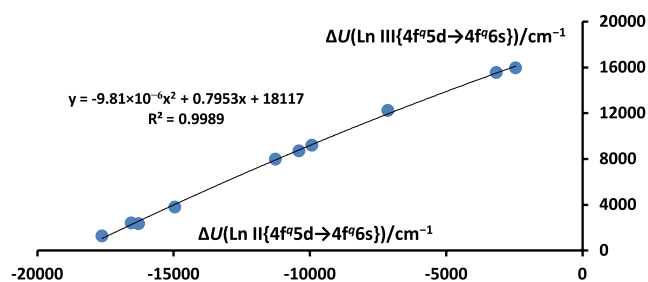


Fig. 4. Experimentally determined differences between the lowest levels of the $4f^q 5d$ and $4f^q 6s$ configurations in Ln III spectra plotted against their iso-electronic Ln II counterparts. The data appear in Table 3.

Pm III, and Sm III, respectively. The complete set of $4f^q 5d \rightarrow 4f^q 6s$ transition energies in lanthanide III spectra appears in column 4 of Table 7. The three values obtained from Fig. 4 are placed in parentheses to mark the fact that they are estimates. By doubling the standard deviation of the separations of the points from the curve in Fig. 4, we obtain an uncertainty in the three estimates of $\pm 370 \text{ cm}^{-1}$.

Values of $E(4f^q 6s)$ for Nd III, Pm III, and Sm III can now be obtained using the SD values in column 3 of Table 7. In Nd III the lowest *observed* level of the $4f^3 5d$ configuration is 5K_5 at $15\,262 \text{ cm}^{-1}$ but in the isoelectronic spectrum Pr II, it is 5L_6 which lies about 200 cm^{-1} below 5K_5 and has not yet been identified in Nd III. Ryabchikova *et al.*¹⁴ give a parameterized treatment of the Nd III spectrum which estimates that 5L_6 will lie at about $15\,300 \text{ cm}^{-1}$. The energy of the lowest level of the $4f^3 5d$ configuration cannot be very different from that of 5K_5 and we have placed it at $15\,200 \text{ cm}^{-1}$ with an uncertainty of $\pm 200 \text{ cm}^{-1}$. This is 800 cm^{-1} below the estimate given by Martin.¹⁰

Values for Pm III and Sm III have been obtained by updating Martin's Table 1. This contains SD(I), the energy difference between the lowest levels of $4f^{q+1} 6s^2$ and $4f^q 5d 6s^2$, and SD(III), the difference between the lowest levels of $4f^{q+1}$ and $4f^q 5d$. When more recent, accurate values for praseodymium and gadolinium are added to Martin's Table 1, $\Delta(\text{III}, \text{I})$, the difference $\{\text{SD(III)} - \text{SD(I)}\}$ increases from 8400 cm^{-1} in praseodymium to 8600 cm^{-1} in gadolinium. We interpolate 8400 cm^{-1} in promethium and 8500 cm^{-1} in samarium. The resulting SD estimates for Pm III and Sm III then become our adopted values of $16\,400 \text{ cm}^{-1}$ and $24\,000 \text{ cm}^{-1}$, respectively. They are in only slight disagreement with the view⁵ that the Sm III value lies "a little above $24\,000 \text{ cm}^{-1}$."

The estimated values of $E(4f^q 6s)$ for Nd III, Pm III, and Sm III in column 5 of Table 7 are then the sums of the figures in columns 3 and 4. The fact that they are estimates is marked by placing them in parentheses. The uncertainties in $E(4f^q 6s)$ are obtained by combining the doubled standard deviation obtained from Fig. 4 ($\pm 370 \text{ cm}^{-1}$) with the uncertainty in the SD. Earlier, we took $\pm 200 \text{ cm}^{-1}$ as the uncertainty in the SD of Nd III. For Pm III and Sm III, the SD values are based on Martin's revised estimates.³ In four cases, the standard deviation of their differences from subsequent experimental values was $\pm 530 \text{ cm}^{-1}$. We double this figure and take $\pm 1060 \text{ cm}^{-1}$ as the uncertainty of the SD for Pm III and Sm III. The uncertainties in $E(4f^q 6s)$ are then $\pm 430 \text{ cm}^{-1}$ for Nd III and $\pm 1200 \text{ cm}^{-1}$ for Pm III and Sm III.

6. The Values of $E(4f^q 6s)$ in Ln IV

In the lanthanide spectra Ln IV, $E(4f^q 6s)$ is the energy of the lowest level of the $4f^q 6s$ configuration relative to the $4f^{q+1}$ ground state of the tripositive ion.

In their paper in 1973, Sugar and Reader had available four experimental values of $E(4f^q 6s)$: those of cerium, praseodymium, lutetium, and hafnium. As with the Ln III spectra, they obtained estimates of the eleven missing values by using the system difference (SD). However, in eleven of the fourteen spectra, experimental values of the SD were unavailable. The eleven values were therefore estimated by adding $57\,300 [1000] \text{ cm}^{-1}$ to Martin's estimates¹⁰ for the iso-electronic systems in Ln III.

With these Ln IV SDs, they were able to calculate four values of the transition $4f^q 5d \rightarrow 4f^q 6s$ from their four values of $E(4f^q 6s)$. A nearly linear variation was observed when the four values in Ln IV were plotted against the values for the isoelectronic systems in Ln III. The missing values of the transition $4f^q 5d \rightarrow 4f^q 6s$ in Ln IV were then derived from this variation using the iso-electronic estimated/experimental values in Ln III. When added to the estimated SD values, an estimate of each missing value of $E(4f^q 6s)$ was obtained.

Here then, unknown values of $E(4f^q 6s)$ are obtained by summation of two steps which are themselves usually estimates. This exposes the calculation to the compounding of uncertainties which, in the case of Ln IV spectra, are increased by the assumption that the SDs can be obtained by adding a constant difference to iso-electronic Ln III values. However, it is possible to eliminate the two-step summation. Inclusion of Hf IV now gives us nine experimental values of $E(4f^q 6s)$: cerium,⁴ praseodymium,⁴ neodymium,¹⁵ terbium,¹⁶ erbium,¹⁷ thulium,¹⁸ ytterbium,⁷ lutetium,⁴ and hafnium.^{19,20} In the Ln IV spectra, the ground state configuration is $4f^{q+1}$. In such cases, $E(4f^q 6s)$ is identical to the energy difference between the lowest levels of the configurations $4f^{q+1}$ and $4f^q 6s$. An estimation curve can therefore be established simply by plotting the experimental values of the transition $4f^{q+1} \rightarrow 4f^q 6s$ in Ln IV against those of

TABLE 4. Experimental data used to estimate unknown values of $E(4f^q 6s)$ in Ln IV spectra. In all but one case, the transition energies shown are equal to $E(4f^q 6s)$ because the ground state configuration of the spectrum is $4f^{q+1}$. The exception is Gd III ($q = 7$) where Gd^{2+} has a $4f^7 5d$ ground state and $E(4f^7 6s)$ is 9195 cm^{-1}

q	Ln III{ $4f^{q+1} \rightarrow 4f^q 6s$ } ^a	Ln IV{ $4f^{q+1} \rightarrow 4f^q 6s$ } ^a
	cm ⁻¹	
1	19 236	100 259
2	28 399	110 056 ^b
7	6 814	84 955
10	21 824	10 1710 ^c
11	19 316	98 973 ^d
12	25 303	106 011 ^e
13	34 656	116 798

^aUnless otherwise stated, transition energies occur between the lowest levels of the configurations and data are from Ref. 4.

^bReference 15.

^cReference 17.

^dReference 18.

^eReference 7.

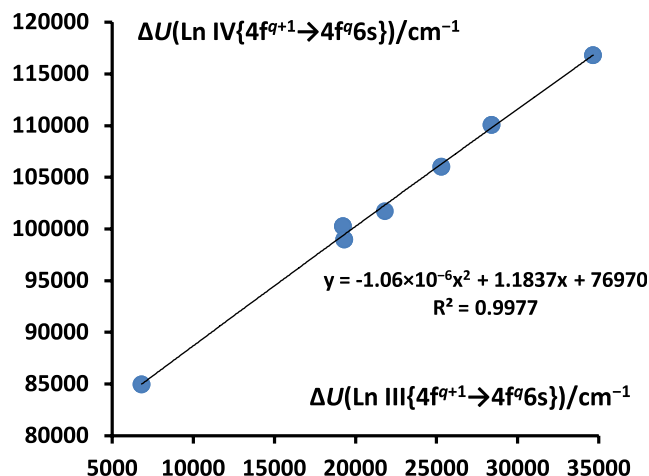


FIG. 5. Differences between the lowest levels of the $4f^{q+1}$ and $4f^q6s$ configurations in the Ln IV spectra plotted against their Ln III counterparts. The data appear in Table 4 (a linear fit gives $y = 1.1434x + 77\,312$).

the iso-electronic Ln III spectra. The data are shown in Table 4. The plot appears in Fig. 5. By means of Fig. 5, missing values of Ln IV $\{E(4f^q6s)\}$ can be estimated from the energies of the transition $4f^{q+1} \rightarrow 4f^q6s$ in Ln III which, in all but two cases, have been determined experimentally. The results are shown in column 3 of Table 8 where the estimates are enclosed in parentheses. For Gd IV, Dy IV, and Ho IV, the uncertainties in $E(4f^q6s)$ are obtained by doubling the sample standard deviations of the points from the curve in Fig. 5. This gives $\pm 1100\text{ cm}^{-1}$. For Pm IV, Sm IV, and Eu IV, we must include a contribution from the values for Nd III, Pm III, and Sm III that were determined in Sec. 5, and upon which they depend. The resulting uncertainties in $E(4f^q6s)$ are $\pm 1200\text{ cm}^{-1}$, $\pm 1600\text{ cm}^{-1}$, and $\pm 1600\text{ cm}^{-1}$, respectively.

7. The Values of G_3 and δ

The lowest energy level arising from a configuration $4f^qns$ when $0 < q < 14$ is one of a pair; it has a partner level arising from the same $4f^q$ parent. The quantity δ is the separation of the lowest level of $4f^qns$ from the unperturbed center of gravity of the pair. In Paper I, Judd's formulae^{8,9} were used to calculate values of δ , which depend on the Racah parameter G_3 , and, with Sugar and Reader,² we found the constant value $G_3 = 210\text{ cm}^{-1}$ to be a satisfactory approximation for $4f^q6s$ in Ln II spectra. When dealing with $4f^q6s$ in the Ln III spectra, Sugar and Reader³ again assumed a constant value ($G_3 = 310\text{ cm}^{-1}$); for the Ln IV spectra they took $G_3 = 410\text{ cm}^{-1}$. However, subsequently

TABLE 6. Values of the Racah parameter $G_3(4f^q7s)$ that were used in calculating the ΔT values plotted in Figs. 1 and 2

Spectrum	Ce III ^a	Gd III ^b	Er III ⁶	Yb III ^a	Pr IV ^c	Yb IV ⁷	Lu IV ²⁷
G_3/cm^{-1}	82	101	98	104	(104)	135	73

^aCalculated from the $4f(2F)7s$ levels using Judd's formulae.

^bCalculated from the $4f(8S)7s$ levels following Wybourne.⁹

^cEstimated; see Sec. 8.2.

parameterized analyses of the spectra suggest significant variation in the Ln III and Ln IV cases. In Table 5 we give values of G_3 obtained from experimental data by analyses of this kind. These appear without parentheses. For both Ln III and Ln IV, the terminal values are larger than the initial ones, but there is a minimum close to the middle of the series near the half-filled shell configuration $4f^76s$. To obtain estimates for the missing values, we have assumed linear changes between the experimental values and the resulting estimates appear in parentheses. With the exceptions of Pr III, Eu III, and Gd IV, values of δ for the lowest level of the $4f^q6s$ configuration are then given by Judd's first formula^{8,9} which puts δ equal to S_1G_3 . Here S_1 is the total spin quantum number of the $4f^q$ core. In Pr III, we accepted Sugar and Reader's analysis³ based on $4f(2^3H)ns$ centers of gravity. This implies $\delta = 292\text{ cm}^{-1}$. In Eu III and Gd IV, the lowest level of the $4f^q6s$ configuration with $J = 1/2$ is perturbed by interaction with a close but higher level that has the same value of J . In these two cases, we have simply modified Sugar and Reader's calculation by calculating δ with our revised estimates of G_3 in Table 5. For Eu III and Gd IV, we found 758 cm^{-1} and 851 cm^{-1} , respectively. The complete sets of δ values for $4f^q6s$ appear in Tables 7 and 8. The sources for G_3 in Table 5 provide typical uncertainties of $\pm 20\text{ cm}^{-1}$ in Ln III spectra and $\pm 30\text{ cm}^{-1}$ in Ln IV. We multiply these figures by S_1 to get the consequent uncertainties in δ .

Finally, some values of $G_3(4f^q7s)$ are needed for the calculation of the ΔT values plotted in Figs. 1 and 2. The non-zero values appear in Table 6.

8. The Ionization Energies

Column 5 of Table 7 contains values of $E(4f^q6s)$ that were obtained in the way described in Sec. 5. The two subsequent columns in Table 7 provide the additional data needed to convert them into the third ionization energies that appear in the last two columns of the table, the first giving figures in cm^{-1} and the second in eV. Table 8 gives the values of $E(4f^q6s)$ obtained in Sec. 6 and repeats the operations of Table 7 to give the fourth

TABLE 5. Values of the Racah parameter G_3 for the configuration $4f^q6s$ in Ln III and Ln IV spectra. Estimated values are in parentheses. The other values were obtained from analyses of experimentally determined spectra

Ln III	Ce ^a	Pr ²¹	Nd	Pm	Sm	Eu ²²	Gd ^b	Tb ²³	Dy ¹²	Ho ²⁴	Er ⁶	Tm ^c	Yb ²⁵
G_3/cm^{-1}	313	309	(307)	(305)	(302)	299	294	278	303	313	303	295	337
Ln IV	Pr ²⁶	Nd ¹⁵	Pm	Sm	Eu	Gd	Tb ^b	Dy	Ho	Er ¹⁷	Tm ¹⁸	Yb ⁷	Lu ²⁷
G_3/cm^{-1}	384	390	(378)	(365)	(352)	(339)	327	(348)	(369)	391	409	419	437

^aCalculated from the $4f(2F)6s$ levels using Judd's formulae.

^bCalculated from the $4f(8S)6s$ levels following Wybourne.⁹

^cCalculated from the $4f(2^3H)6s$ levels using Judd's formulae.

TABLE 7. Calculation of I_3 using Fig. 4 for the estimation of unknown values of $E(4f^q6s)$

q		SD ^a	$4f^q5d \rightarrow 4f^q6s^a$	$E(4f^q6s)^a$	δ	$T(4f^q6s)$	I_3	I_3/eV
		cm^{-1}						
0	La	0	13 591	13 591	0	141 086	154 677	19.178
1	Ce	3 277	15 959	19 236	157	143 516	162 909	20.198
2	Pr	12 847	15 553	28 399	292	145 719	174 410	21.624
3	Nd	(15 200) ^b	(14 872) ^b	(30 072) ^b	461	147 606	178 139	22.086
4	Pm	(16 400) ^b	(14 394) ^b	(30 794) ^b	610	149 589	180 993	22.440
5	Sm	(24 000) ^b	(13 598) ^b	(37 598) ^b	755	151 564	189 917	23.547
6	Eu	33 856	12 240	46 096	758	153 531	200 385	24.845
7	Gd	0	9 195	9 195	1029	155 425	165 649	20.538
8	Tb	8972	8 704	17 676	834	157 454	175 964	21.817
9	Dy	16 453 ^c	7 980 ^c	24 433 ^c	758	159 422	184 613	22.889
10	Ho	18 033	3 791	21 824	626	161 374	183 824	22.791
11	Er	16 976	2 340	19 316	455	163 348	183 159	22.704
12	Tm	22 897	2 405	25 303	295	165 265	190 863	23.664
13	Yb	33 386	1 270	34 656	169	167 243	202 068	25.053
14	Lu	5 708	−5 708	0	0	169 047	169 047	20.959

^aUnless otherwise stated, transitions occur between the lowest levels of the configurations; data are from Ref. 4.

^bEstimated values, see text.

^cReference 12.

TABLE 8. Calculation of I_4 from the experimental values of $E(4f^q6s)$ and estimated values obtained using Fig. 5

q		$E(4f^q6s)^a$	δ	$T(4f^q6s)$	I_4	I_4/eV
		cm^{-1}				
0	Ce	86 602	0	211 069	297 671	36.907
1	Pr	100 259	192	214 086	314 537	38.998
2	Nd	110 056 ^b	390	217 017	327 463	40.600
3	Pm	(111 604) ^c	567	219 852	332 023	41.166
4	Sm	(112 412) ^c	730	222 695	335 837	41.639
5	Eu	(119 970) ^c	880	225 497	346 347	42.942
6	Gd	(129 282) ^c	851	228 320	358 453	44.443
7	Tb	84 955	1145	231 111	317 211	39.329
8	Dy	(97 562) ^c	1044	233 955	332 561	41.232
9	Ho	(105 259) ^c	923	236 799	342 981	42.524
10	Er	101 710 ^b	782	239 624	342 116	42.417
11	Tm	98 973 ^b	614	242 446	342 033	42.407
12	Yb	106 011 ^b	419	245 281	351 711	43.607
13	Lu	116 798	219	247 943	364 960	45.249
14	Hf	18 380 ^d	0	250 762	269 142	33.369

^aUnless otherwise stated, data are from Ref. 4.

^bSee references in Table 4.

^cEstimated from Fig. 5; see text.

^dReference 19.

ionization energies in its last two columns. In Table 9, our third and fourth ionization energies are compared with those estimated by Sugar and Reader (1973)³ and with the current NIST recommendations.⁴

The uncertainties in our ionization energies were calculated by combining those in $T(4f^q6s)$, $E(4f^q6s)$, and δ in quadratic fashion. The figures for the three components appear in Secs. 2–7.

8.1. Third ionization energies

The NIST values for La, Ce, Pr, Yb, and Lu are identical to ours because they have small uncertainties and were used as basic data in our semiempirical scheme. In these cases, differences from Sugar and Reader³ are due to subsequent

improvements that are independent of the methods used both by them and in this paper.

For the five elements Gd, Tb, Ho, Er, and Tm, the NIST values are virtually identical to those of Sugar and Reader and, in these cases, NIST does indeed cite the 1973 paper as the source. The differences in europium and dysprosium are due to improved spectroscopic data obtained since 1973,^{11,12} which allowed recalculations of I_3 using Sugar and Reader's method and auxiliary data. Until recently, the NIST database also recommended Sugar and Reader's third ionization energies for Nd, Pm, and Sm. However, during the preparation of this paper, it introduced the new figures in column 3 of Table 9.

The revised NIST values for neodymium and samarium are those of Morss²⁸ who derived them from thermo-chemical cycles. The method is exposed to uncertainties in auxiliary thermodynamic data, including those in the values of lanthanide second ionization energies for which Morss used the estimates of Sugar and Reader² that we have since recalculated. Nevertheless, his values for the third ionization energies of neodymium and samarium agree with ours within the range of uncertainties.

In promethium, the NIST database currently recommends the value obtained by Vander Sluis and Nugent.²⁹ This is 0.4 eV lower than ours and lies well outside our uncertainty range. In the middle region of the series, Vander Sluis and Nugent's linearization technique produces values of the third ionization energies that are lower than those found by other methods. In neodymium and samarium, their estimates are 0.2 and 0.36 eV lower than the current NIST values. Similar deficiencies of 0.13–0.26 eV occur in Eu, Gd, Tb, and Dy. Vander Sluis and Nugent suggested that this might be because the interpolations made by Sugar and Reader did not take account of what we have called the subshell break. However, our revision eliminates this problem, and the disparities with Vander Sluis and Nugent's method persist.

To summarize, if we ignore the case of promethium, our values differ from the NIST recommendations by less than 0.1 eV, being slightly lower from samarium onward.

TABLE 9. Three sets of third and fourth ionization energies: Columns 2 and 6, Sugar and Reader (1973); columns 3 and 7, current NIST recommendations; columns 4 and 8, this work

Element	I_3/eV			Element	I_4/eV		
	S&R 1973	NIST 2016	This work		S&R 1973	NIST 2016	This work
La	19.1774[6]	19.1773[6]	19.1773[6]	Ce	36.758[5]	36.906[9]	36.906[9]
Ce	20.198[3]	20.1974[25]	20.1974[25]	Pr	38.98[2]	38.981[25]	39.00[8]
Pr	21.624[3]	21.6237[25]	21.6237[25]	Nd	40.41[20]	40.4[4]	40.60[8]
Nd	22.14[30]	22.05[11]	22.09[8]	Pm	41.09[32]	41.0[6]	41.17[17]
Pm	22.32[36]	22.04[13]	22.44[15]	Sm	41.37[38]	41.4[7]	41.64[21]
Sm	23.43[30]	23.56[11]	23.55[15]	Eu	42.65[32]	42.7[6]	42.94[21]
Eu	24.70[32]	24.92[10]	24.84[6]	Gd	44.01[35]	44.0[7]	44.44[16]
Gd	20.63[10]	20.63[10]	20.54[6]	Tb	39.79[20]	39.36[10]	39.33[8]
Tb	21.91[10]	21.91[10]	21.82[6]	Dy	41.47[20]	41.4[4]	41.23[16]
Dy	22.79[30]	22.93[10]	22.89[6]	Ho	42.48[32]	42.5[6]	42.52[16]
Ho	22.84[10]	22.84[10]	22.79[6]	Er	42.65[21]	42.7[4]	42.42[8]
Er	22.74[10]	22.74[10]	22.70[6]	Tm	42.69[20]	42.7[4]	42.41[8]
Tm	23.68[10]	23.68[10]	23.66[6]	Yb	43.74[20]	43.56[10]	43.61[8]
Yb	25.03[2]	25.053[25]	25.053[25]	Lu	45.19[2]	45.249[25]	45.249[25]
Lu	20.9596[10]	20.9594[12]	20.9594[12]	Hf	33.33[2]	33.370[25]	33.370[25]

8.2. Fourth ionization energies

Again, the identity of the NIST values for Ce, Lu, and Hf with ours reflects their low uncertainties and their use in our fitting procedures.

For the 11 elements Pr–Gd and Dy–Yb, the NIST database again cites Sugar and Reader (1973)³ as the source. In terbium, the difference of 0.43 eV between Sugar and Reader's value and that cited by NIST is important because it arises from subsequent work¹⁶ that identified $E(4f^7 6s)$ at 84 955 cm^{-1} , compared with the estimate of 88 100 cm^{-1} in the 1973 paper. The chief source of the error was the $4f^n \rightarrow 4f^q 5d$ system difference which was found at 51 404 cm^{-1} rather than 54 900 cm^{-1} . Our value for terbium differs from the revised NIST estimate by only 0.03 eV.

In the first half of the series, between neodymium and gadolinium, our estimated values exceed the NIST recommendations by 0.17–0.44 eV. In the second half of the series, between dysprosium and thulium, our values tend to be lower, but by less than 0.3 eV. One effect of these last differences is that the three-quarter shell effect, the downward break in I_4 between holmium and thulium, is more pronounced. The NIST data suggest that the value in thulium is 0.2 eV greater than in holmium; our values imply that it is 0.1 eV less. It may be that an important contribution to the differences arises from Sugar and Reader's use of a constant difference in the SDs of Ln III and Ln IV spectra. Spector and Sugar's later revision in terbium,¹⁶ which reduced the ionization energy by 0.4 eV, suggested that this was the case. It also led them to recommend a doubling of the uncertainties proposed by Sugar and Reader for the nine elements Nd–Gd and Dy–Tm. This recommendation seems to have been accepted by NIST. Our estimation method avoids the use of SD and has an improved auxiliary database. Consequently, throughout the series the uncertainties in our estimated values are smaller than those proposed by NIST, except at praseodymium. This exception is chiefly due to our uncertainty in Δn^* (± 0.005) which is more than double that proposed by Sugar and Reader.³

A recent paper³⁰ has drawn attention to the discrepancy of 3000 cm^{-1} between the NIST value for the fourth ionization

energy of praseodymium (38.98 eV) and the quantum mechanical value of Eliav *et al.* (38.61 eV).³¹ It suggests that Sugar and Reader's semi-empirical value might be at fault because of an aberrant value of Δn^* brought on by configuration interaction between $4f7s$ and $5d6p$ levels. The same suggestion automatically applies to our retracing of Sugar and Reader's method which has yielded a value close to theirs (39.00 eV).

Unfortunately, most of the $4f7s$ and $5d6p$ levels in Pr IV have not been experimentally observed. This makes the assessment of configuration interaction difficult. The upper level of $4f(2F_{5/2})7s$ ($J = 3$) occurs at 199 728 cm^{-1} but the lower level ($J = 2$) is missing. We have used the estimate, $G_3 = 104 \text{ cm}^{-1}$, taken from Yb IV and Lu IV, to place it at 199 640 cm^{-1} . Of the 11 levels of $5d6p$, only two have been observed: $3F_4$ at 195 917 cm^{-1} and $1F_3$ at 202 487 cm^{-1} . However, these estimates and observations do suggest that the full set spans the two relevant levels of $4f7s$ and this supports the possibility of a strong configuration interaction.

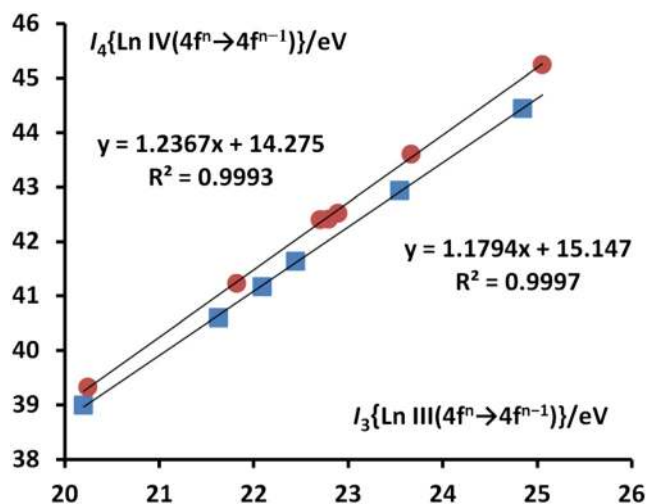


FIG. 6. The fourth ionization energies of the lanthanides plotted against the third ionization energies for isoelectronic transitions of the type $\{\text{Xe}\}4f^n \rightarrow \{\text{Xe}\}4f^{n-1}$. The lower plot shows the sequence Ce III/Pr IV \rightarrow Eu III/Gd IV; the upper plot shows Gd III/Tb IV \rightarrow Yb III/Lu IV.

The proximity of the levels of the two configurations depends on the charge of the ion, and in the isoelectronic Ce III, the 5d6p levels all lie above those of 4f7s. For example, there are separations of 3000 cm⁻¹ between 4f(²F_{5/2})7s (*J* = 2) and 5d6p(³F₂), and 6400 cm⁻¹ between 4f(²F_{5/2})7s (*J* = 3) and 5d6p(³F₃). In this case, larger separations would weaken any configuration interaction but if it occurs, it should have suppressed ΔT and, in its absence, the ionization energy would be higher. There is, however, no obvious sign of this. As Fig. 6 shows, plots of our values of I_4 against the isoelectronic values for I_3 (corrected in Gd²⁺ to a 4f^{*n*} ground state) show excellent linearity for the sequences Ce III/Pr IV → Eu III/Gd IV and Gd III/Tb IV → Yb III/Lu IV. The R^2 values are 0.9997 and 0.9993, respectively. There is therefore no indication that the value for Pr(IV) is markedly aberrant in the context of the other semiempirical values.

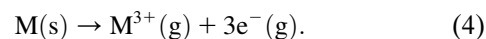
Finally we note that, since the work of Eliav *et al.*, other quantum mechanical calculations have been made. Those of Cao and Dolg³² treated the lanthanide series as a whole and this less specific approach by two slightly different methods gave values of 38.84 and 39.04 eV, which closely span those given by NIST and by us. Clearly there is a need for further work on the problem and especially on the spectrum of Pr IV.

8.3. The standard enthalpies of formation of gaseous tripositive ions

This quantity is needed for the calculation of the lattice enthalpies of lanthanide compounds and the hydration enthalpies of ions. It can also be used to explore the possibility of a subshell break and to check the overall reliability of our estimates. It can be calculated from the equation

$$\Delta_f H^\ominus(M^{3+}, g) = \Delta_f H^\ominus(M, g) + I_1 + I_2 + I_3 + (15/2)RT. \quad (3)$$

Here we use the familiar ideal gas standard state at a pressure of 1 bar for gaseous ions and electrons. There are two recent reviews of the values of $\Delta_f H^\ominus(M, g)$ for the lanthanide elements.^{33,34} We have used the averages of the two sets, and they appear in column 3 of Table 10. Promethium has been omitted because of the absence of an experimental value. When combined with the NIST values of I_1 , which have small uncertainties,⁴ and our revised values of I_2 and I_3 , Eq. (3) gives the values of $\Delta_f H^\ominus(M^{3+}, g)$ in column 4. $\Delta_f H^\ominus(M^{3+}, g)$ refers to the reaction



Most lanthanide metals have some form of hexagonal close-packed structure³³ with three bonding electrons per metal atom outside an inner 4f^{*n*} sub-shell.³⁵ Reaction (4) is then one in which the 4f electrons are conserved. The energies of this kind of reaction usually vary nearly smoothly across the lanthanide series. This is because coupling between the outer bonding and inner 4f electrons is weak. There may be perturbations of the smooth variation caused by structural variations or a tetrad effect^{36–38} but these are usually small (≤ 4 kJ mol⁻¹).

In Fig. 7, $\Delta_f H^\ominus(M^{3+}, g)$ has been plotted against q , the number of 4f electrons in the gaseous tripositive ion. The cerium value has been increased by 2 kJ mol⁻¹ to place it in the β hexagonally close packed form.^{33,34} Eleven of the fourteen values vary nearly smoothly with q , any deviations from the curve being ≤ 8 kJ mol⁻¹ and less than the experimental uncertainties cited in Table 10. Two of the three

TABLE 10. Thermodynamic data on lanthanide compounds and ions at 298.15 K; q is the number of 4f electrons in the gaseous tripositive ion

q	Element	$\Delta_f H^\ominus(M, g)^a$	$\Delta_f H^\ominus(M^{3+}, g)^b$	$\Delta_f H^\ominus(MCl_3, s)^c$	$\Delta_f H^\ominus(M^{3+}, aq)^d$	$\Delta_f H^\ominus(M_2O_3, s)^e$
kJ mol ⁻¹						
0	La	432.3[40]	3918[4]	-1071.6[15]	-707.6[25]	-1791.6[20]
1	Ce	428.4[30]	3987[5]	-1059.9[15]	-702.4[20]	-1799.8[10]
2	Pr	356.2[30]	4015[5]	-1058.1[15]	-705.7[20]	-1809.9[30]
3	Nd	326.5[20]	4050[9]	-1041.0[10]	-694.8[20]	-1806.9[30]
5	Sm	206.7[20]	4111[15]	-1025.3[20]	-690.0[20]	-1826.8[50]
6	Eu	178.0[20]	4227[7] ^f	-935.4[30]	-605.4[40]	-1662.5[60]
7	Gd	401.5[50]	4160[9]	-1020.8[30]	-698.4[20]	-1819.7[40]
8	Tb	389.7[30]	4190[8]	-1010.6[30]	-699.8[40]	-1865.2[60]
9	Dy	286.9[30]	4211[8]	-992.8[30]	-700.2[30]	-1863.4[50]
10	Ho	302.9[40]	4238[8]	-997.6[25]	-707.7[30]	-1883.3[80]
11	Er	313.6[40]	4262[8]	-995.0[20]	-708.2[30]	-1900.1[70]
12	Tm	232.8[30]	4295[8]	-996.3[25]	-711.1[30]	-1889.3[60]
13	Yb	152.1[20]	4366[4]	-959.4[30]	-676.3[30]	-1814.5[60]
14	Lu	427.6[30]	4355[10]	-985.7[25]	-703.3[30]	-1877.0[80]

^aAverages of the sets of values recommended in Refs. 33 and 34.

^bCalculated from Eq. (3) with first ionization energies from Ref. 4 and the recommended second and third ionization energies from Parts 1 and 2 of this work.

^cAverage of the set of values recommended in Refs. 40 and 41.

^dReference 43.

^eReference 42.

^fIncludes an electronic contribution to ($H_{298}^\ominus - H_0^\ominus$) for Eu³⁺(g) of 1.7 kJ mol⁻¹.

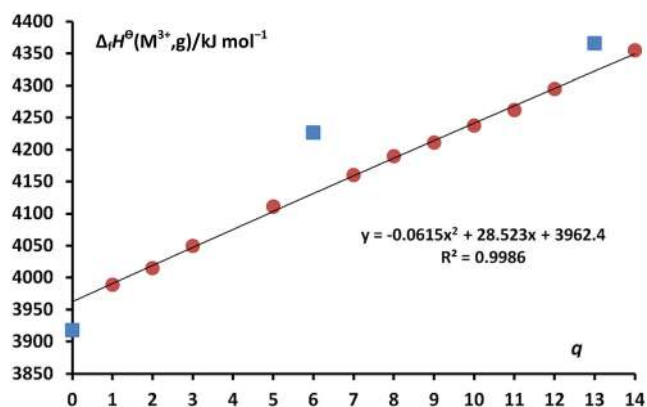


FIG. 7. Plot of $\Delta_f H^\ominus(M^{3+},g)$ for lanthanide elements against q where q is the number of 4f electrons in the gaseous tripositive ion. The polynomial fit covers only the dark red circular points. The square points represent lanthanum, europium, and ytterbium; promethium has been omitted.

exceptions, those in europium and ytterbium, are displaced upward by 96 and 43 kJ mol^{-1} , respectively. This is because in these two metals, there are two bonding electrons, rather than three, outside an inner $4f^{q+1}$ subshell.³⁵ The displacements represent the amounts by which the two-electron divalent metals are stabilized with respect to the three-electron trivalent state. The third exception is in lanthanum which is displaced downward by 45 kJ mol^{-1} . We regard the good fit observed for eleven trivalent metals in Fig. 7 and the large displacement at $q = 0$ as support for both our revised ionization energies and a substantial subshell break.

8.4. Irregularities in the $4f^q 5d \rightarrow 4f^{q+1} 6s$ transition in Ln III

In Sec. 5, we required values of the differences between the lowest levels of this transition for Nd III, Pm III, and Sm III. We obtained them by plotting known values for Ln III spectra against their isoelectronic Ln II counterparts. Figure 3 plots the

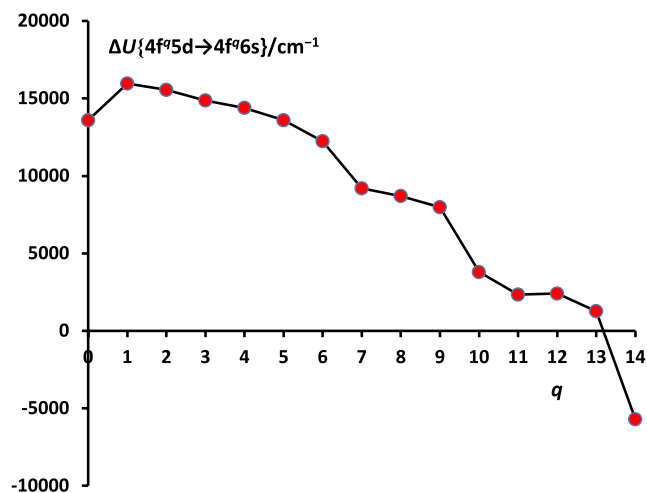


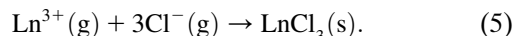
FIG. 8. Variations in the energy of the transition between the lowest levels of the $4f^q 5d$ and $4f^{q+1} 6s$ configurations in lanthanide III spectra plotted against q . The values at $q = 3, 4,$ and 5 have been estimated from Fig. 4.

data that we used and it includes the complete variation for Ln II with an incomplete one for Ln III. In Fig. 8 we have added our estimated values and plotted a complete variation for Ln III.

In this transition, the 4f electrons are conserved but unlike other changes of this type (Figures 1, 2, and 7) the transition energy does not vary nearly smoothly between $4f^1$ and $4f^{14}$. It seems that the 5d electron couples much more strongly with the inner $4f^q$ subshell than do the s electrons in Figs. 1 and 2 or the bonding electrons in lanthanide metals. It is noticeable that the pattern of the irregularities in Fig. 8 is that of a tetrad effect, which, while only slightly evident in the first half of the series, is prominent from $q = 6$ onward: the values at f^7 , f^{10} , and f^{11} are depressed with respect to their immediate neighbors. This suggests that a substantial contribution to the irregularities is made by an increase in the interelectronic repulsion energy within the 4f subshell when the outer electron moves out of the 5d and into the 6s orbital.³⁶⁻³⁸ According to the theory of the tetrad effect, this increase varies irregularly across the series and generates downward breaks at f^3/f^4 , f^7 , and f^{10}/f^{11} . However, in this case, the irregularities are an order of magnitude greater than those found in familiar examples of the effect which involve conventional chemical reactions.³⁹

8.5. Lattice enthalpies and hydration enthalpies of trivalent compounds and ions

Here we find out if the subshell break in our values of $\Delta_f H^\ominus(M^{3+},g)$ is transmitted to lattice enthalpies and hydration energies. Reviews of the enthalpies of formation of lanthanide trichlorides,^{40,41} sesquioxides,⁴² and aqueous ions⁴³ give the values shown in Table 10. The figures for the trichlorides are the averages of those in Refs. 40 and 41. We take the lattice enthalpy of a solid lanthanide trichloride, $L^\ominus(\text{LnCl}_3)$, to be the standard enthalpy change, at 298.15 K, of the reaction



Thus, $L^\ominus(\text{LnCl}_3,\text{s})$ is given by

$$L^\ominus(\text{LnCl}_3,\text{s}) = \Delta_f H^\ominus(\text{LnCl}_3,\text{s}) - \Delta_f H^\ominus(\text{Ln}^{3+},\text{g}) - 3\Delta_f H^\ominus(\text{Cl}^{-},\text{g}). \quad (6)$$

Demonstrations of a subshell break are more convincing if they avoid possible irregularities introduced by structural change. We can do this by using the seven trichlorides, $\text{LaCl}_3 \rightarrow \text{GdCl}_3$, which all have the hexagonal UCl_3 structure⁴⁰ (PmCl_3 has been omitted). With data from columns 4 and 5 of Table 10, and the value⁴⁴ $\Delta_f H^\ominus(\text{Cl}^{-},\text{g}) = -233.95 \text{ kJ mol}^{-1}$, Eq. (6) yields the values of $L^\ominus(\text{LnCl}_3)$ plotted in Fig. 9(A). The subshell break is 36 kJ mol^{-1} .

There is evidence that in the early part of the lanthanide series, the four aqueous ions, $\text{La}^{3+}(\text{aq})$, $\text{Ce}^{3+}(\text{aq})$, $\text{Pr}^{3+}(\text{aq})$, and $\text{Nd}^{3+}(\text{aq})$, all have nine-fold trigonal tri-prismatic coordination.⁴⁵ We can reproduce the variations in the hydration enthalpies of these ions by using the quantity $\{\Delta_f H^\ominus(M^{3+},\text{aq}) - \Delta_f H^\ominus(M^{3+},\text{g})/\text{kJ mol}^{-1}\}$ calculated from columns 4 and 6 of Table 10. This has been done in Fig. 9(B). The subshell break is 33 kJ mol^{-1} .

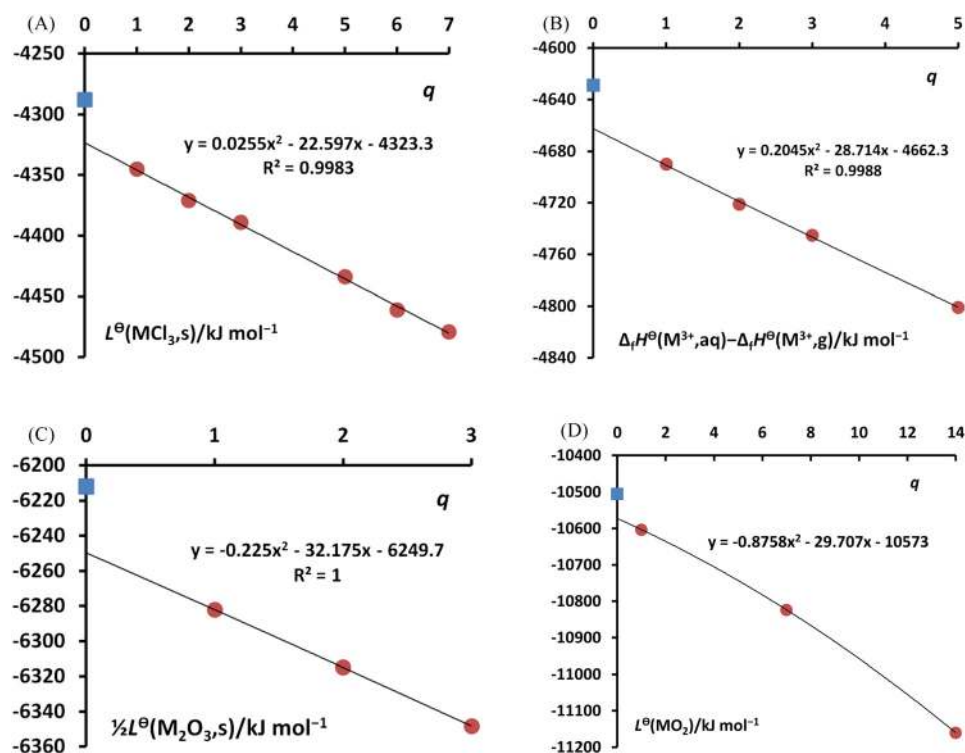


FIG. 9. The lattice and hydration enthalpies of some isostructural trivalent and tetravalent lanthanide compounds and ions plotted against q , the number of 4f electrons in the free ion. (A) The lattice enthalpies of trichlorides; (B) the variation in the hydration enthalpies of tripositive ions; (C) the lattice enthalpies of sesquioxides; (D) the lattice enthalpies of dioxides. Points in the range $q = 1 \rightarrow 14$ are marked with dark red circles; the $q = 0$ point is marked with a blue square.

TABLE 11. Calculation of the lattice enthalpies of lanthanide and hafnium dioxides with the fluorite structure; q is the number of 4f electrons in the gaseous tetrapositive ion

q	Element	$\Delta_t H^\ominus(\text{M}, \text{g})$ kJ mol ⁻¹	$\Delta_t H^\ominus(\text{M}^{4+}, \text{g})$ kJ mol ⁻¹	$\Delta_t H^\ominus(\text{MO}_2, \text{s})$ kJ mol ⁻¹	$L^\ominus(\text{MO}_2, \text{s})^a$ kJ mol ⁻¹
0	Ce	428.4[30] ^b	7554[6] ^c	-1090.4[10] ^d	-10 505
1	Pr	356.2[30] ^b	7784[10] ^c	-959.1[20] ^d	-10 603
7	Tb	389.7[30] ^b	7991[12] ^c	-972.2[50] ^d	-10 823
14	Hf	618.4[60] ^c	8207[60] ^e	-1093[11] ^f	-11 160

^aCalculated using Eq. (8) with $\Delta_t H^\ominus(\text{O}^{2-}, \text{g}) = 930 \text{ kJ mol}^{-1}$.

^bSee Table 10.

^cCalculated from Eq. (7) with first ionization energies from Ref. 4 and the recommended second, third, and fourth ionization energies from Parts 1 and 2 of this work.

^dReference 42.

^eReference 44.

^fCalculated from Eq. (7) with ionization energies from Ref. 4.

^gReference 57 with an adjustment for conversion to a fluorite structure; see text.

The sesquioxides of the series $\text{La}_2\text{O}_3 \rightarrow \text{Nd}_2\text{O}_3$ all have the hexagonal A-type M_2O_3 structure.⁴² The values of $\frac{1}{2}L^\ominus(\text{Ln}_2\text{O}_3)$ can be calculated from columns 4 and 7 of Table 10 and the estimated value $\Delta_t H^\ominus(\text{O}^{2-}, \text{g}) = 930 \text{ kJ mol}^{-1}$.⁴⁶ Since this estimate is a constant for each lattice enthalpy, it does not affect the variation, or the subshell break of 38 kJ mol^{-1} revealed by Fig. 9(C).

8.6. Lattice enthalpies of tetravalent lanthanide oxides

Past investigations of the first transition series have found that the subshell break tends to increase with the oxidation state of

the transition element.^{47–50} Does this also occur in the lanthanide series? The experimental data are very limited but seem sufficient to answer this question. In the series $\text{Ce} \rightarrow \text{Hf}$, there are just four known dioxides: those of cerium, praseodymium, terbium, and hafnium. The dioxides of the first three elements have the eight-coordinate fluorite structure.⁴² At room temperature, hafnium dioxide has a monoclinic structure in which the hafnium atom is seven-coordinate. However, the cubic fluorite form is stable above 2870 K and there is an experimental value of 5.08 \AA for its unit cell parameter⁵¹ (internuclear distance 2.20 \AA). Theoretical calculations^{52–56} indicate that, at 298.15 K, the standard enthalpy of the change from the monoclinic to the fluorite structure is approximately $25 \pm 10 \text{ kJ mol}^{-1}$. The value

of $\Delta_f H^\ominus(\text{HfO}_2, \text{monoclinic})$ ⁵⁷ is $-1117.5 \pm 2 \text{ kJ mol}^{-1}$ so we use the figure $\Delta_f H^\ominus(\text{HfO}_2, \text{fluorite}) = -1093 \pm 11 \text{ kJ mol}^{-1}$.

Table 11 contains the enthalpies of formation of the other three dioxides.⁴² The quantity $\Delta_f H^\ominus(\text{M}^{4+}, \text{g})$ and the lattice enthalpy, $L^\ominus(\text{MO}_2, \text{s})$, can be calculated from the equations

$$\Delta_f H^\ominus(\text{M}^{4+}, \text{g}) = \Delta_f H^\ominus(\text{M}, \text{g}) + I_1 + I_2 + I_3 + I_4 + 10RT, \quad (7)$$

$$L^\ominus(\text{MO}_2, \text{s}) = \Delta_f H^\ominus(\text{MO}_2, \text{s}) - \Delta_f H^\ominus(\text{M}^{4+}, \text{g}) - 2\Delta_f H^\ominus(\text{O}^{2-}, \text{g}). \quad (8)$$

For the three lanthanide elements, we have used our revised ionization energies and the $\Delta_f H^\ominus(\text{M}, \text{g})$ values given earlier in this paper. The ionization energies of hafnium and its enthalpy of atomization are taken from Refs. 4 and 44. The lattice enthalpies were again calculated using $\Delta_f H^\ominus(\text{O}^{2-}, \text{g}) = 930 \text{ kJ mol}^{-1}$ and, in Fig. 9(D), they are plotted against q . The subshell break amounts to 68 kJ mol^{-1} , approximately double that observed for the oxides $1/2\text{M}_2\text{O}_3$. It can be seen from Fig. 9(D) that the relative positions of the CeO_2 , PrO_2 , and TbO_2 points are such that the size of the break is relatively insensitive to the large uncertainties in the hafnium data.

9. Conclusion

The improvements in the auxiliary data, and the modifications that we have made to earlier estimation methods, justify the revised ionization energies and uncertainties listed in Table 9. The ionization energies with higher uncertainties mark the absence of desirable information from the observed spectra, notably the missing energies of the lowest levels of $4f^9 6s$ for $\text{Nd III} \rightarrow \text{Sm III}$, $\text{Nd IV} \rightarrow \text{Gd IV}$, Dy IV , and Ho IV . In Pm III and Sm III , the uncertainties are further enhanced by the absence of values for the SD. Thus, further work on all these spectra could improve the estimation scheme. Finally two specific ionization energies, along with their associated spectra, merit further experimental investigation. First, the fourth ionization energy of praseodymium, obtained through the estimation scheme used by both us and Sugar and Reader, has been questioned from a theoretical standpoint. Second, we take this opportunity to reaffirm the point made in Paper I: the study of lanthanide systematics would be especially helped by a more accurate experimental value of the second ionization energy of lutetium.

Acknowledgments

As in the case of Paper I, the authors are very grateful for the extensive criticisms and suggestions made by a reviewer.

10. References

- D. A. Johnson and P. G. Nelson, *J. Phys. Chem. Ref. Data* **46**, 013108 (2017).
- J. Sugar and J. Reader, *J. Opt. Soc. Am.* **55**, 1286 (1965).
- J. Sugar and J. Reader, *J. Chem. Phys.* **59**, 2083 (1973).
- A. Kramida, Y. Ralchenko, J. Reader, and NIST ASD Team, NIST Atomic Spectra Database version 5.4 [Online] (National Institute of Standards and Technology, Gaithersburg, MD, 2016), available: <http://physics.nist.gov/asd>.
- W. C. Martin, R. Zalubas, and L. Hagan, *Atomic Energy Levels—The Rare Earth Elements* (National Bureau of Standards, Washington, DC, 1978).
- J.-F. Wyart, J. Blaise, W. P. Bidelman, and C. R. Cowley, *Phys. Scr.* **56**, 446 (1997).
- J.-F. Wyart, W. L. Tchang-Brillet, N. Spector, P. Palmeri, P. Quinet, and E. Biemont, *Phys. Scr.* **63**, 113 (2001).
- B. R. Judd, *Phys. Rev.* **125**, 613 (1962).
- B. G. Wybourne, *Spectroscopic Properties of Rare Earths* (Interscience, New York, 1965), pp. 53–56.
- W. C. Martin, *J. Opt. Soc. Am.* **61**, 1682 (1971).
- J. Sugar and N. Spector, *J. Opt. Soc. Am.* **64**, 1484 (1974).
- N. Spector, J. Sugar, and J.-F. Wyart, *J. Opt. Soc. Am. B* **14**, 511 (1997).
- L. Brewer, *J. Opt. Soc. Am.* **61**, 1666 (1971).
- T. Ryabchikova, A. Ryabtsev, O. Kochukhov, and S. Bagnulo, *Astron. Astrophys.* **456**, 329 (2006).
- J.-F. Wyart, A. Meftah, W. L. Tchang-Brillet, N. Champion, O. Lamrous, N. Spector, and J. Sugar, *J. Phys. B* **40**, 3957 (2007).
- N. Spector and J. Sugar, *J. Opt. Soc. Am.* **66**, 436 (1976).
- A. Meftah, S. A. Mammari, J.-F. Wyart, W.-Ü. L. Tchang-Brillet, N. Champion, C. Blaess, D. Deghiche, and O. Lamrous, *J. Phys. B* **49**, 165002 (2016).
- A. Meftah, J.-F. Wyart, N. Champion, and W. L. Tchang-Brillet, *Eur. Phys. J. D* **44**, 35 (2007).
- P. F. A. Klinkenberg, T. A. M. van Kleef, and P. E. Noorman, *Physica* **27**, 151 (1961).
- J. Sugar and V. Kaufman, *J. Opt. Soc. Am.* **64**, 1656 (1974).
- J. Sugar, *J. Opt. Soc. Am.* **53**, 831 (1963).
- J.-F. Wyart, W.-Ü. L. Tchang-Brillet, S. S. Churilov, and A. N. Ryabtsev, *Astron. Astrophys.* **483**, 339 (2008).
- E. Meinders, Th. A. M. Van Kleef, and J.-F. Wyart, *Physica* **61**, 443 (1972).
- J.-F. Wyart, H. M. Crosswhite, and R. Hussain, *Physica C* **85**, 386 (1977).
- B. W. Bryant, *J. Opt. Soc. Am.* **55**, 771 (1965).
- J. Sugar, *J. Opt. Soc. Am.* **55**, 1058 (1965).
- J. Sugar and V. Kaufman, *J. Opt. Soc. Am.* **62**, 562 (1972).
- L. R. Morss, *Chem. Rev.* **76**, 827 (1976).
- K. L. Vander Sluis and L. J. Nugent, *J. Chem. Phys.* **60**, 1927 (1974).
- V. A. Dzuba, M. S. Safronova, U. I. Safronova and A. Kramida, *Phys. Rev. A* **94**, 042503 (2016).
- E. Eliav, U. Kaldor, and Y. Ishikawa, *Phys. Rev. A* **51**, 225 (1995).
- X. Cao and M. Dolg, *Mol. Phys.* **101**, 961 (2003).
- R. J. M. Konings and O. Benes, *J. Phys. Chem. Ref. Data* **39**, 043102 (2010).
- J. W. Arblaster, in *Handbook on the Physics and Chemistry of the Rare Earths*, edited by J.-C. G. Bunzli and V. K. Pecharsky (North Holland, Amsterdam, 2013), Vol. **43**, pp. 321–565.
- D. A. Johnson, *J. Chem. Soc. A* **1969**, 1525.
- C. K. Jorgensen, *J. Inorg. Nucl. Chem.* **32**, 3127 (1970).
- L. J. Nugent, *J. Inorg. Nucl. Chem.* **32**, 3485 (1970).
- D. A. Johnson, in *Inorganic Chemistry in Focus III*, edited by G. Meyer, D. Naumann and L. Wesemann (Wiley-VCH, Weinheim, 2006), p. 1.
- D. F. Peppard, C. A. Bloomquist, E. P. Horowitz, S. Lewey, and G. W. Mason, *J. Inorg. Nucl. Chem.* **32**, 339 (1970).
- E. H. P. Cordfunke and R. J. M. Konings, *Thermochim. Acta* **375**, 17 (2001).
- A. D. Chervonnyi, in *Handbook on the Physics and Chemistry of the Rare Earths*, edited by J.-C. G. Bunzli and V. K. Pecharsky (North Holland, Amsterdam, 2013), Vol. **42**, pp. 165–484.
- R. J. M. Konings, O. Benes, A. Kovacs, D. Manara, D. Sedmidubsky, L. Gorokhov, V. S. Iorish, V. Yungman, E. Shenyavskaya, and E. Osina, *J. Phys. Chem. Ref. Data* **43**, 013101 (2014).
- E. H. P. Cordfunke and R. J. M. Konings, *Thermochim. Acta* **375**, 51 (2001).
- M. W. Chase, *NIST-Janaf Thermochemical Tables*, 4th ed. (American Institute of Physics, New York, 1998).
- D. A. Johnson and P. G. Nelson, *Inorg. Chem.* **51**, 6116 (2012).

- ⁴⁶D. A. Johnson, *Some Thermodynamic Aspects of Inorganic Chemistry*, 2nd ed. (Cambridge University Press, Cambridge, England, 1982), p. 41.
- ⁴⁷D. A. Johnson and P. G. Nelson, *Inorg. Chem.* **34**, 3253 (1995).
- ⁴⁸D. A. Johnson and P. G. Nelson, *Inorg. Chem.* **34**, 5666 (1995).
- ⁴⁹D. A. Johnson and P. G. Nelson, *J. Chem. Soc., Dalton Trans.* **1995**, 3483.
- ⁵⁰D. A. Johnson and P. G. Nelson, *Inorg. Chem.* **38**, 4949 (1999).
- ⁵¹J. Wang, H. P. Li, and R. Stevens, *J. Mater. Sci.* **27**, 5397 (1992).
- ⁵²A. S. Foster, F. Lopez Gejo, A. L. Shluger, and R. Nieminen, *Phys. Rev. B* **65**, 174117 (2002).
- ⁵³J. Kang, E. C. Lee, and K. J. Chang, *Phys. Rev. B* **68**, 054106 (2003).
- ⁵⁴J. E. Jaffe, R. A. Bachorz, and M. Gutowski, *Phys. Rev. B* **72**, 144107 (2005).
- ⁵⁵J. I. Beltran, M. C. Munoz, and J. Hafner, *New J. Phys.* **10**, 063031 (2008).
- ⁵⁶X. Luo, W. Zhou, S. V. Ushakov, A. Navrotsky, and A. A. Demkov, *Phys. Rev. B* **80**, 134119 (2009).
- ⁵⁷A. N. Kornilov, I. M. Ushakova, E. J. Huber, and C. E. Holley, *J. Chem. Thermodyn.* **7**, 21 (1975).